Cell Reports, Volume *42*

Supplemental information

Premature aging and reduced cancer incidence associated with near-complete body-wide *Myc* inactivation

Huabo Wang, Jie Lu, Taylor Stevens, Alexander Roberts, Jordan Mandel, Raghunandan Avula, Bingwei Ma, Yijen Wu, Jinglin Wang, Clinton Van't Land, Toren Finkel, Jerry E. Vockley, Merlin Airik, Rannar Airik, Radhika Muzumdar, Zhenwei Gong, Michel S. Torbenson, and Edward V. Prochownik

Fig. S1

A

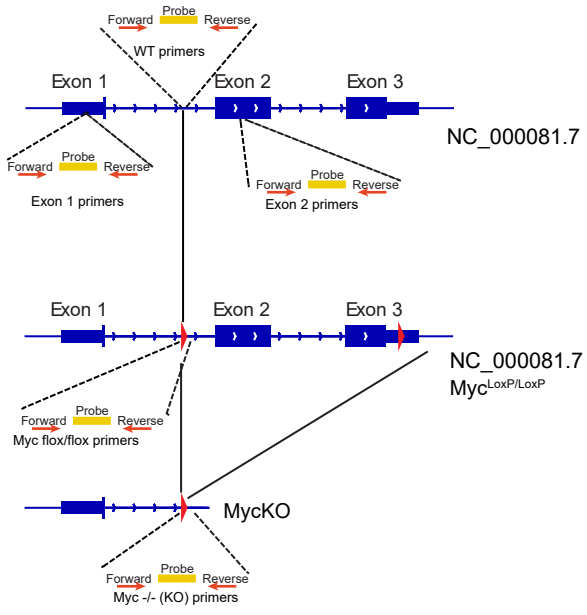

B

C

D

		Start (bp)	End (bp)	Sequence (5' -3')
WT (NC_000081.7)	Forward	61858492	61858513	GGGAATCCTCACATTCCTACTT
	Reverse	61858643	61858626	GATTCAGCACTGGGTGCA
	Probe	61858549	61858572	/56-FAM/TAGGAAGACTGCGGTGAGTCGTGA/3IABkFQ/
Myc loxP/loxP (NC_000081.7)	Forward	61858570	61858588	TGATCTGAGCGGTTCCGTA
	Reverse	61858697	61858675	CACCTCCCTTCTACACTCTAAAC
	Probe	Loxp	Loxp	/56-FAM/CCTGCACGA/ZEN/TCCGGAACCCTTAAT/3IABkFQ/
Myc -/- (KO) (NC_000081.7)	Forward	61858570	61858588	TGATCTGAGCGGTTCCGTA
	Reverse	61858697	61858675	TAAAGTCCCAAAGACACTCCAG
	Probe	Loxp	Loxp	/56-FAM/CCTGCACGATCCGGAACCCTTAAT/3IABkFQ/
Exon 1 (NC_000081.7)	Forward	61857404	61857425	GCTGTAGTAATTCCAGCGAGAG
	Reverse	61857507	61857488	ACTCCAGAGCTGCCTTCTTA
	Probe	61857447	61857468	/56-FAM/TTGGAAGAG/ZEN/CCGTGTGTCCAGA/3IABkFQ/
Exon 2 (NC_000081.7)	Forward	61859421	61859442	CTCCGTACAGCCCTATTTCATC
	Reverse	61859542	61859524	TGGGAAGCAGCTCGAATTT
	Probe	61859464	61859480	/56-FAM/TATCACCAG/ZEN/CAACAGCA
Cre (OM228709.1)	Forward	3366	3344	GCGGTCTGGCAGTAAAAACTATC
	Reverse	3265	3287	GTGAAACAGCATTGCTGTCACTT
	Probe	3323	3300	/56-FAM/AAACATGCT/ZEN/TCATCGTCGGTCCGG/3IABkFQ/
Rosa WT (NC_000072.7)	Forward	113053072	113053056	CTGGCTTCTGAGGACCG
	Reverse	113052875	113052894	CCGAAAATCTGTGGGAAGTC
	Probe	113052960	113052983	/56-FAM/TTTAAGCCT/ZEN/GCCCAGAAGACTCCC/3IABkFQ/

E

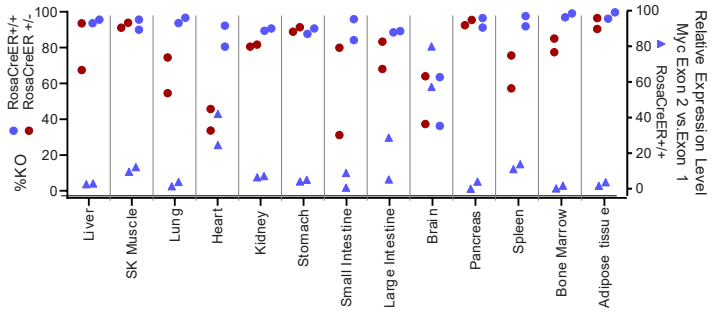

F

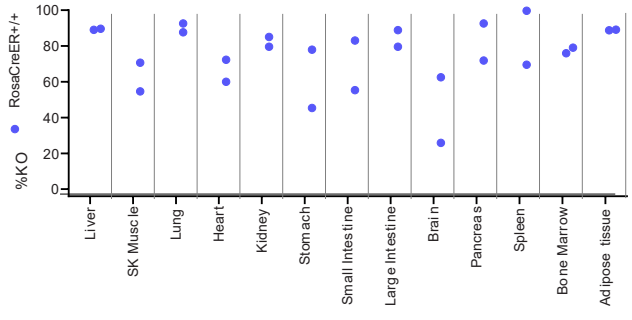

G

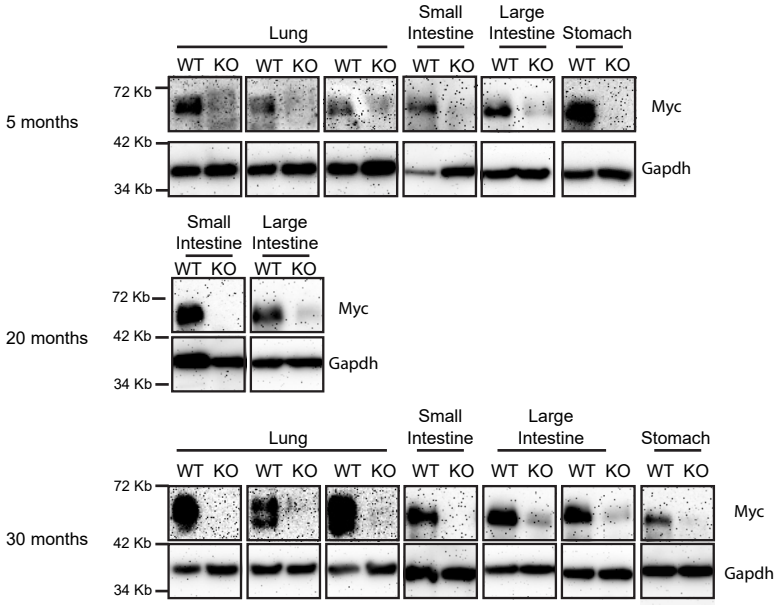

H

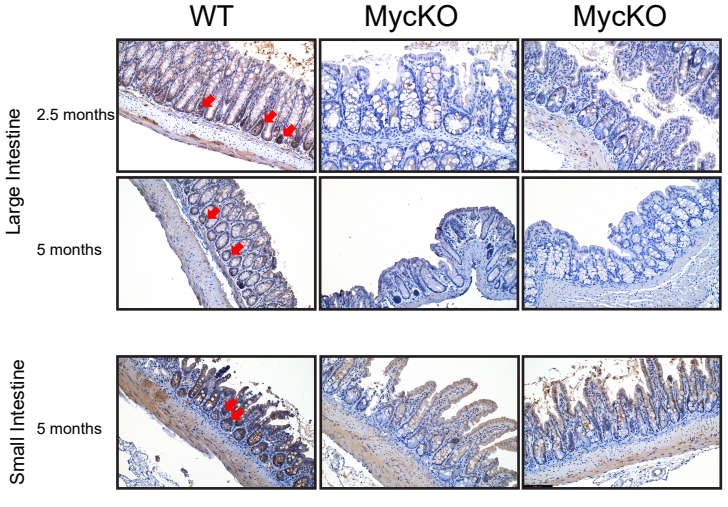

Figure S1. Strategy for qPCR-based Taq-Man-based assay for identifying *Myc* alleles, related to STAR Methods.

(A, B). The *Myc* loci of WT and *myc*$^{loxP/loxP}$ (B6.129S6-*Myc*^{tm2Fwa}/Mmjax) mice. LoxP sites are indicated by red triangles. In A, the red arrows indicate the primer sets used to amplify the WT allele. The reverse primer in intron 1 overlaps the inserted LoxP site in the (*Myc*$^{loxp/loxP}$) allele shown in B. Amplification with this primer set is thus possible only in WT mice and generates a PCR fragment detected with the unique TaqMan probe. In B, red arrows indicate the primer set flanking the 5' LoxP site that specifically amplifies this region and is detected with TaqMan probe.

(C). The excised and recombined *Myc* locus following CreER activation.

(D). Sequences and genomic locations for primers and probes shown in A-C as well as the qRT-PCR primers and probes used for qRT-PCR. Annotations for primers and probes are based on the numbering of the murine genomic sequence: https://www.ncbi.nlm.nih.gov/gene/17869.

(E). qPCR and qRT-PCR-based quantification of *Myc* locus excision and expression in ~6-7 wk old mice that had been treated for 5 days with tamoxifen at the time of weaning (~4 wks and weights >15 g). 2 mice with 2 copies of CreER and 2 with a single copy of CreER were used to determine how *Myc* locus excision efficiency was influenced by CreER copy number. After confirming the number of CreER alleles using the TaqMan-based approach described above, the WT:KO *Myc* allele ratio was determined from a standard curve of known amounts of each DNA (Wang et al., 2018; Wang et al., 2022b)(Wang et al., 2018; Wang et al., 2022b). qRT PCR reactions for Myc transcripts (https://www.ncbi.nlm.nih.gov/gene/17869) were performed on RNAs extracted from tissues of mice with two copies of ROSA-CreER as previously described [1,2].

(F). Persistence of *Myc* locus deletion. qPCR performed as described in E on the indicted tissues from 20-22 month-old *Myc*KO mice. See Table S1 for a summary of qPCR and qRT-PCR results performed on various tissues of additional mice.

(G). Immuno-blotting for Myc protein in the indicated tissues from 5-6 months, 20-22 months and 30-33 months old WT and *Myc*KO mice.

(H). Immunohistochemical staining for Myc protein in the small and large intestines of WT and *Myc*KO mice. Note, in both tissues, the absence of detectable Myc in the crypts which is where the highest levels of expression are confined. [3] Scale bar = 100 μm.

Fig. S2

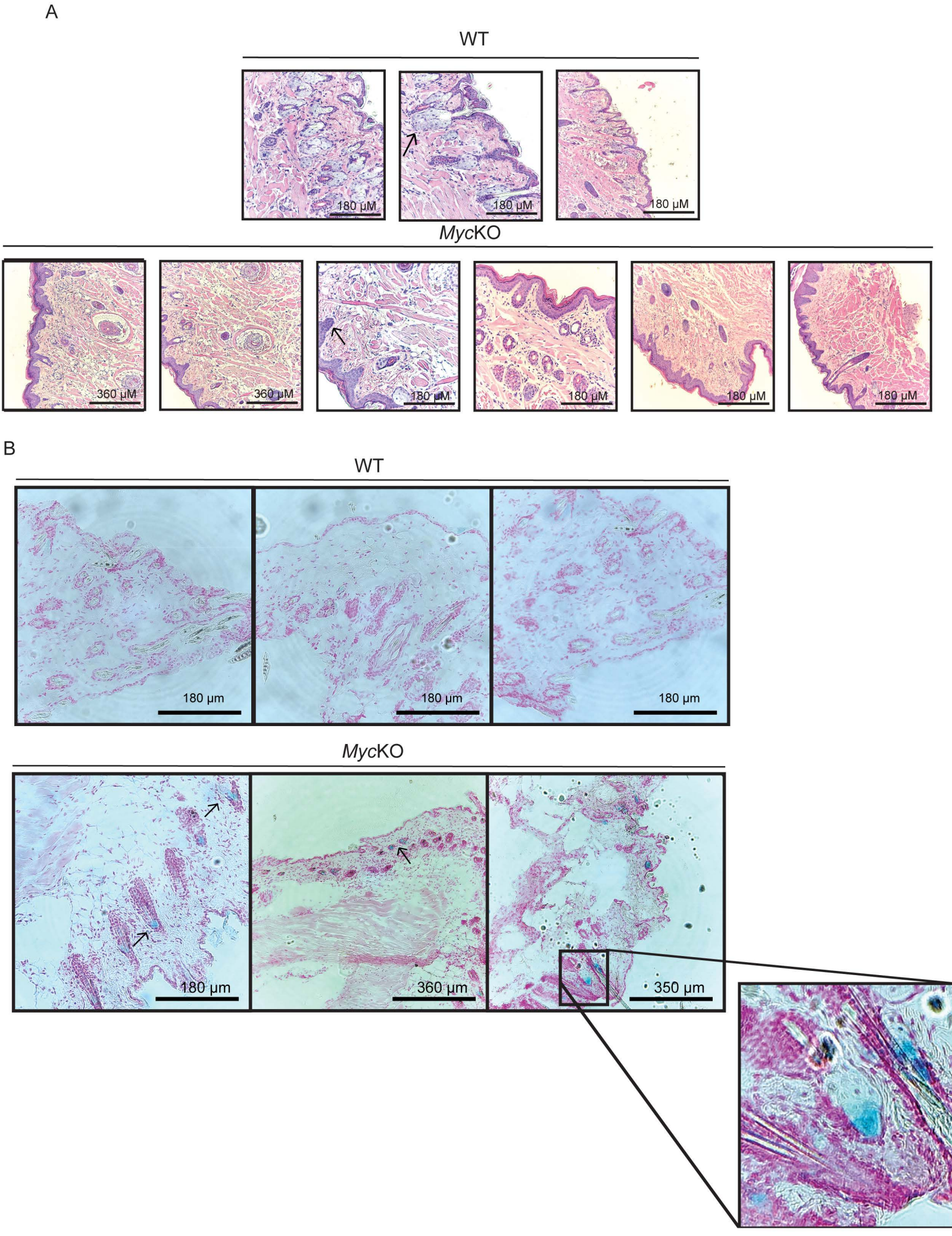
A
WT
180 μM
180 μM
180 μM
MycKO
360 μM
360 μM
180 μM
180 μM
180 μM
180 μM
B
WT
180 μm
180 μm
180 μm
MycKO
180 μm
360 μm
350 μm

Figure S2. Histopathology of skin from alopecic regions of *Myc*KO mice and premature onset of senescence, related to Figure 1B&C.

(A). H&E-stained sections of peri-orbital skin from a 5 mo *Myc*KO mouse and normal skin from the corresponding region of a WT control mouse. In WT panels, the arrow shows normal hair follicles and their adjacent sebaceous glands. In *Myc*KO panels, the arrows show thickening and hyperkeratinization of the epidermis, loss of surface invaginations and a generalized paucity of hair follicles and sebaceous glands. (B). SA-β-gal staining of the same areas from the WT and *Myc*KO mice shown in A. Arrows indicate SA-β-gal-positive cells in the latter samples adjacent to rare hair follicles. Most of SA-β-gal-positive cells detected resided within the inner and outer root sheath and base of the follicle (http://eulep.pdn.cam.ac.uk/~skinbase/). A higher power magnification of one of the fields containing SA-β-gal-positive cells is shown to the right.

Fig. S3

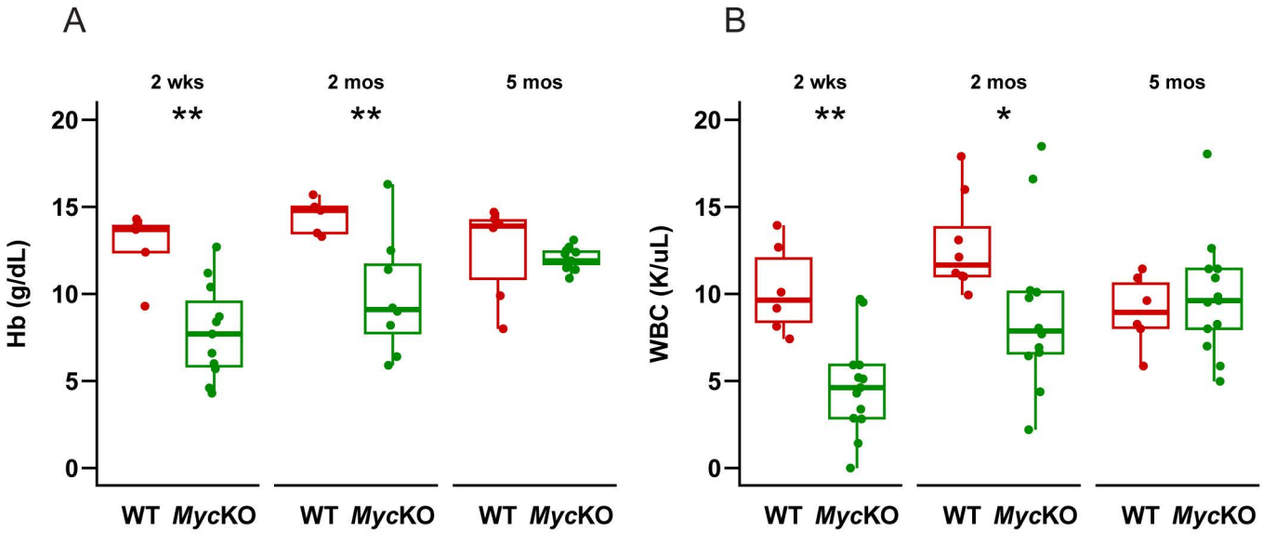
A
2 wks
2 mos
5 mos
**
**
Hb (g/dL)
20
15
10
5
0
WT MycKO
WT MycKO
WT MycKO
B
2 wks
2 mos
5 mos
**
*
WBC (K/uL)
20
15
10
5
0
WT MycKO
WT MycKO
WT MycKO

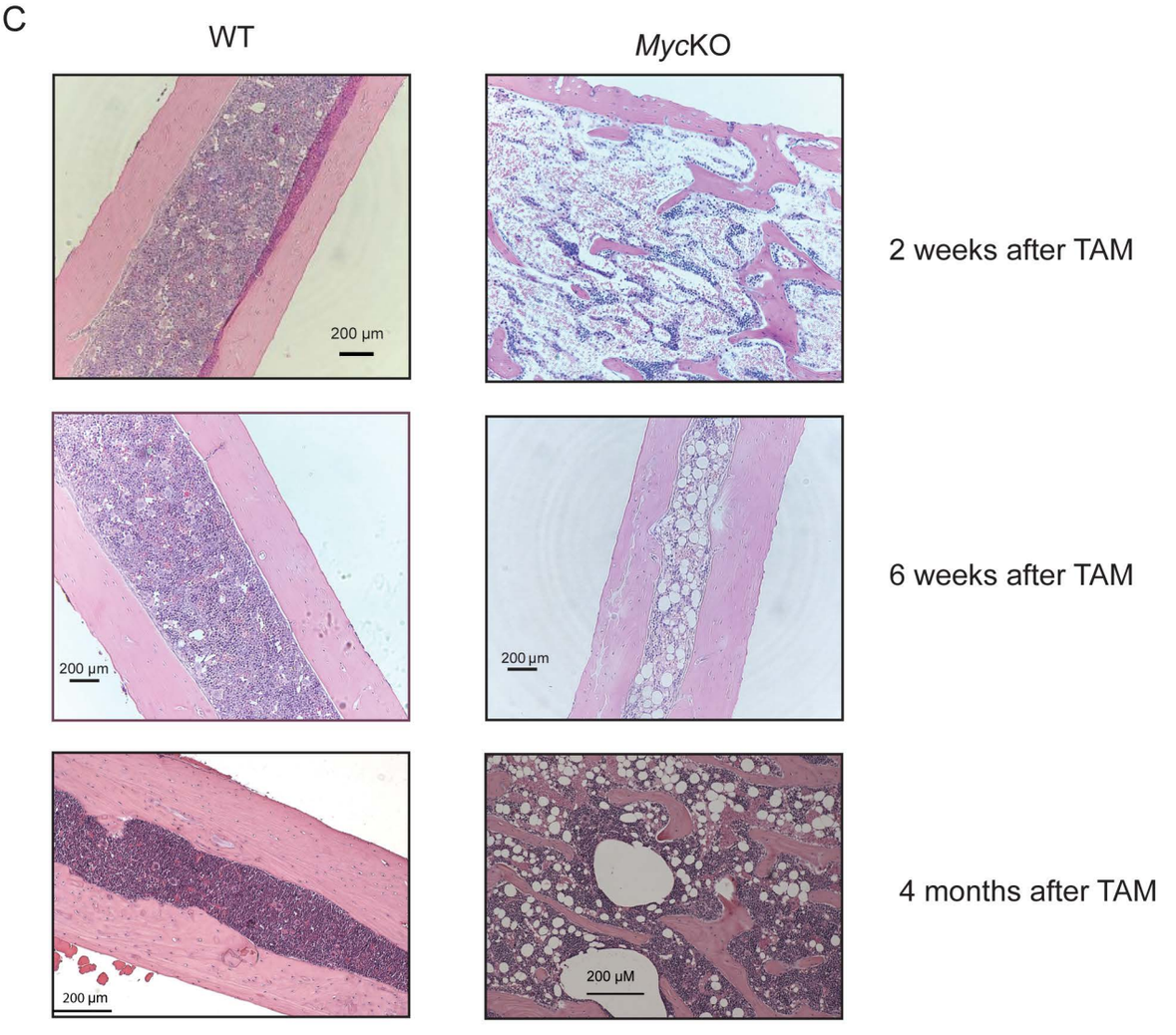
C
WT
MycKO
200 µm
2 weeks after TAM
200 µm
200 µm
6 weeks after TAM
200 µm
200 µM
4 months after TAM

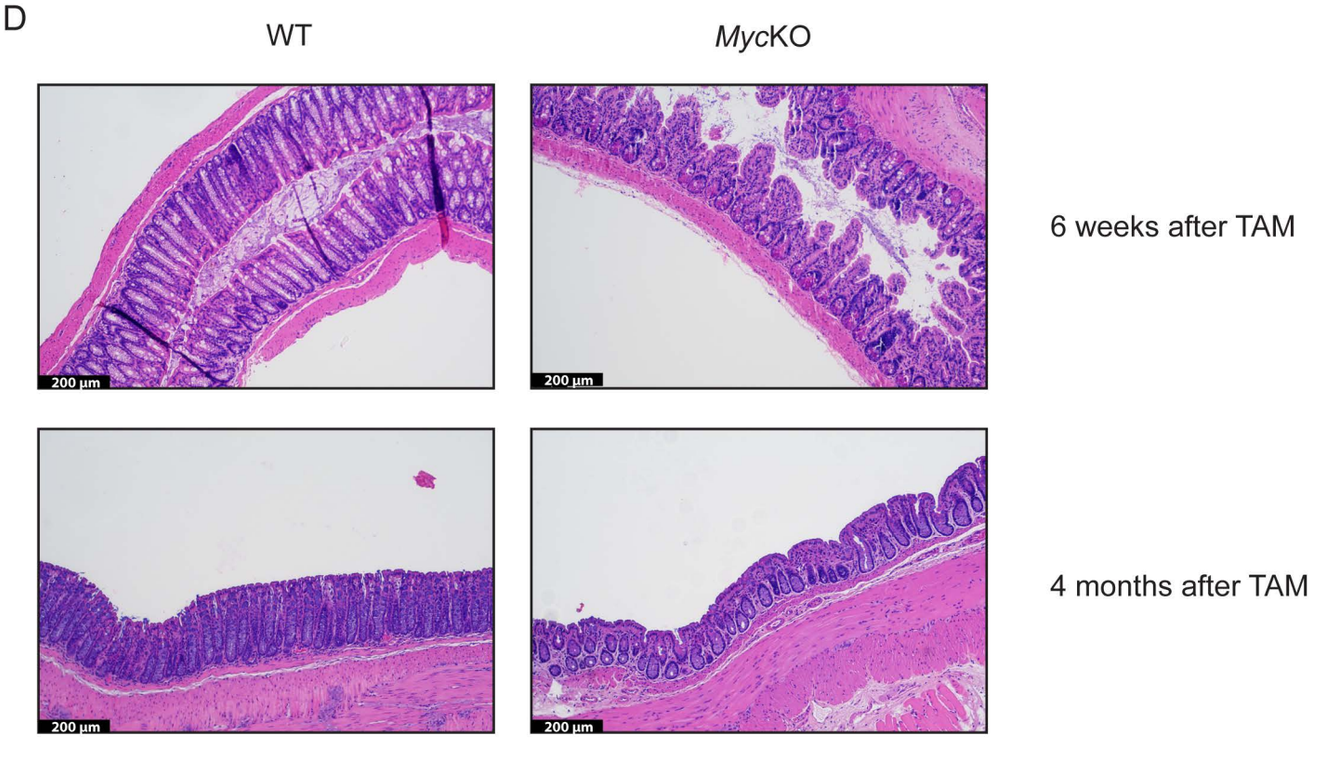
D
WT
MycKO
200 µm
200 µm
6 weeks after TAM
200 µm
200 µm
4 months after TAM

Figure S3. *Myc*KO mice develop transient mild-moderate, anemia, leukopenia and bone marrow hypoplasia, related to Figure 1&3.

(A). Hemoglobin levels in WT and age-matched *Myc*KO mice at the indicated ages, which are expressed relative to the time of starting 4-hydroxytamoxifen therapy. N = 6-14 at each age, Unpaired t test, $*=p < 0.05$, $**=p < 0.01$.

(B). Peripheral white blood cell counts performed at the times shown in A.

(C). H&E-stained bone marrows of WT and *Myc*KO mice of the indicated ages.

(D). H&E-stained colonic tissues from WT and *Myc*KO mice of the indicated ages.

Scale bar = 200 μm

Fig. S4

A

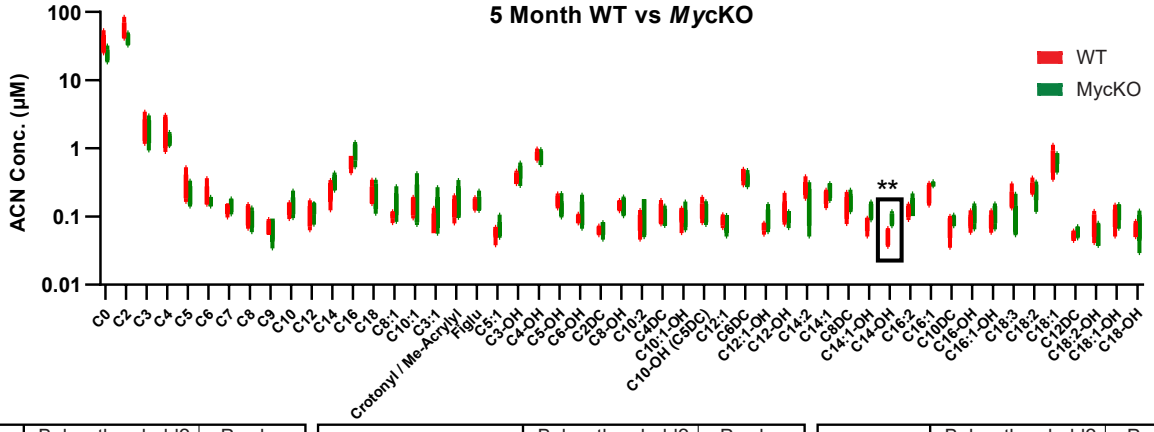

	Below threshold?	P value
C0	No	0.082805
C2	No	0.107371
C3	No	0.891553
C4	No	0.310665
C5	No	0.243173
C6	No	0.395319
C7	No	0.342432
C8	No	0.408316
C9	No	0.932381
C10	No	0.639306
C12	No	0.252238
C14	No	0.123141
C16	No	0.112089
C18	No	0.812097
C8:1	No	0.179578
C10:1	No	0.757984
C3:1	No	0.365815

	Below threshold?	P value
Crotonyl / Me-Acrylyl	No	0.341981
Figlu	No	0.931718
C5:1	No	0.726059
C3-OH	No	0.206181
C4-OH	No	0.735646
C5-OH	No	0.158956
C6-OH	No	0.359565
C2DC	No	0.437708
C8-OH	No	0.815773
C10:2	No	0.357354
C4DC	No	0.519504
C10:1-OH	No	0.495535
C10-OH (C5DC)	No	0.804210
C12:1	No	0.551986
C6DC	No	0.184811
C12:1-OH	No	0.258790
C12-OH	No	0.468176

	Below threshold?	P value
C14:2	No	0.110939
C14:1	No	0.174621
C8DC	No	0.640394
C14:1-OH	No	0.052795
C14-OH	Yes **	0.003299
C16:2	No	0.426658
C16:1	No	0.066959
C10DC	No	0.267349
C16-OH	No	0.179856
C16:1-OH	No	0.179856
C18:3	No	0.093283
C18:2	No	0.605520
C18:1	No	0.788717
C12DC	No	0.268356
C18:2-OH	No	0.243451
C18:1-OH	No	0.368712
C18-OH	No	0.548166

B

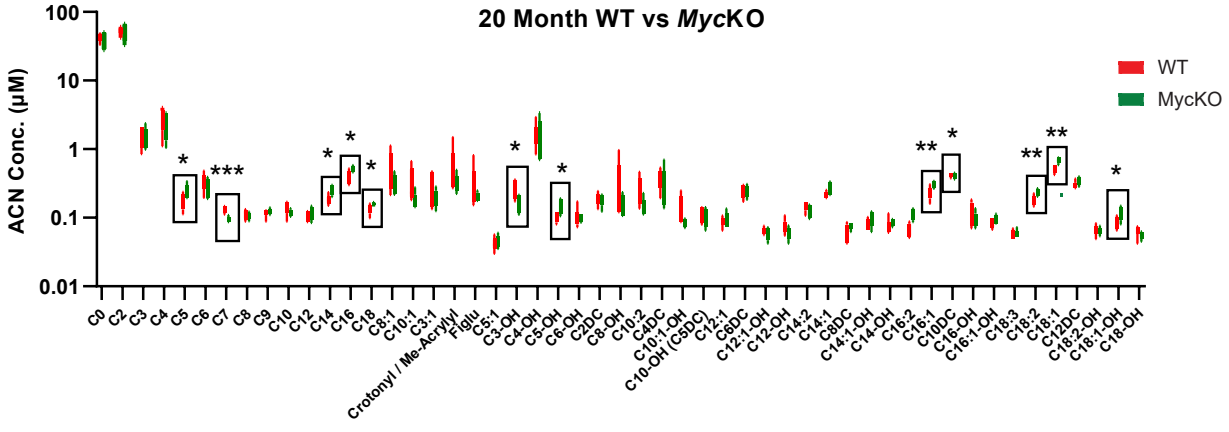

	Below threshold?	P value
C0	No	0.301834
C2	No	0.611193
C3	No	0.856345
C4	No	0.485919
C5	Yes *	0.035634
C6	No	0.260523
C7	Yes ***	0.000783
C8	No	0.497159
C9	No	0.496558
C10	No	0.222842
C12	No	0.359745
C14	Yes *	0.013240
C16	Yes *	0.044914
C18	Yes *	0.037790
C8:1	No	0.319791
C10:1	No	0.124682
C3:1	No	0.442019

	Below threshold?	P value
Crotonyl / Me-Acrylyl	No	0.264035
Figlu	No	0.333312
C5:1	No	0.498076
C3-OH	Yes *	0.016120
C4-OH	No	0.768323
C5-OH	Yes *	0.012020
C6-OH	No	0.996976
C2DC	No	0.720109
C8-OH	No	0.294558
C10:2	No	0.137534
C4DC	No	0.413080
C10:1-OH	No	0.125231
C10-OH (C5DC)	No	0.590178
C12:1	No	0.708297
C6DC	No	0.770883
C12:1-OH	No	0.590031
C12-OH	No	0.130382

	Below threshold?	P value
C14:2	No	0.197887
C14:1	No	0.073848
C8DC	No	0.096298
C14:1-OH	No	0.177224
C14-OH	No	0.335738
C16:2	Yes **	0.003900
C16:1	Yes *	0.014118
C10DC	No	0.686387
C16-OH	No	0.293995
C16:1-OH	No	0.150042
C18:3	No	0.969488
C18:2	Yes **	0.008329
C18:1	Yes **	0.003805
C12DC	No	0.117119
C18:2-OH	No	0.595252
C18:1-OH	Yes *	0.043729
C18-OH	No	0.225025

Figure S4. Young and old *Myc*KO mice show evidence of Complex I defects and more generalized mitochondrial dysfunction, related to Figure 4F&G

(A). 5 month-old mice. The results from Figure 4F are again shown along with the actual values obtained for each serum acyl carnitine. Unpaired t test, $**=p < 0.01$

(B). 20 month-old mice. The results from Figure 4G are again shown along with the actual values obtained for each serum acyl carnitine. Unpaired t test, $*=p < 0.05$, $**=p < 0.01$, $***=p < 0.001$.

Fig. S5

A

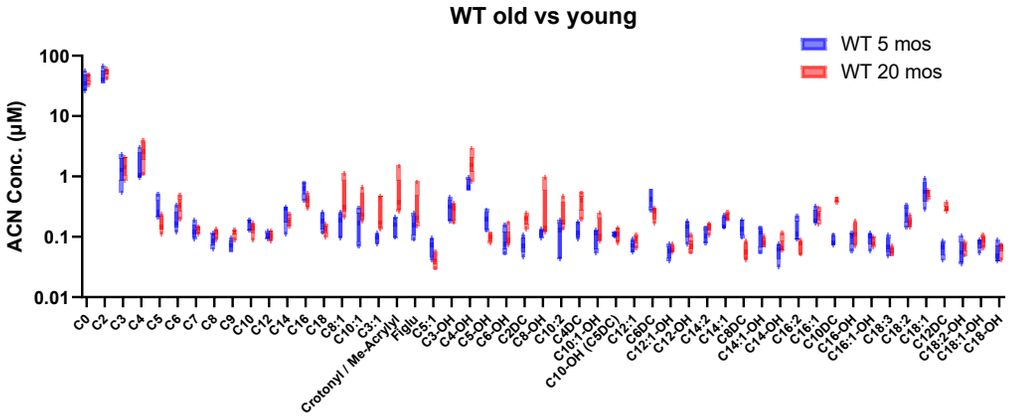

	Below threshold?	P value
C0	No	0.265224
C2	No	0.190087
C3	No	0.774480
C4	No	0.102879
C5	Yes *	0.036385
C6	Yes *	0.027669
C7	No	0.693571
C8	No	0.097887
C9	Yes ***	0.000949
C10	No	0.214036
C12	No	0.969853
C14	No	0.099644
C16	Yes **	0.009118
C18	No	0.055543
C8:1	No	0.083082
C10:1	No	0.124479
C3:1	No	0.050142

	Below threshold?	P value
Crotonyl / Me-Acrylyl	No	0.080009
Figlu	No	0.202828
C5:1	Yes *	0.023385
C3-OH	No	0.708989
C4-OH	Yes *	0.017946
C5-OH	Yes **	0.006523
C6-OH	No	0.612026
C2DC	Yes ***	0.000196
C8-OH	No	0.202814
C10:2	No	0.067778
C4DC	Yes **	0.001957
C10:1-OH	No	0.274583
C10-OH (C5DC)	No	0.879301
C12:1	No	0.084011
C6DC	Yes *	0.014555
C12:1-OH	No	0.372662
C12-OH	Yes **	0.007948

	Below threshold?	P value
C14:2	Yes *	0.024092
C14:1	Yes *	0.035823
C8DC	Yes **	0.001306
C14:1-OH	No	0.173232
C14-OH	No	0.233375
C16:2	Yes *	0.024105
C16:1	No	0.718401
C10DC	Yes ****	<0.000001
C16-OH	No	0.328667
C16:1-OH	No	0.242023
C18:3	No	0.137024
C18:2	No	0.099872
C18:1	No	0.583925
C12DC	Yes ****	<0.000001
C18:2-OH	No	0.493457
C18:1-OH	No	0.419368
C18-OH	No	0.325839

B

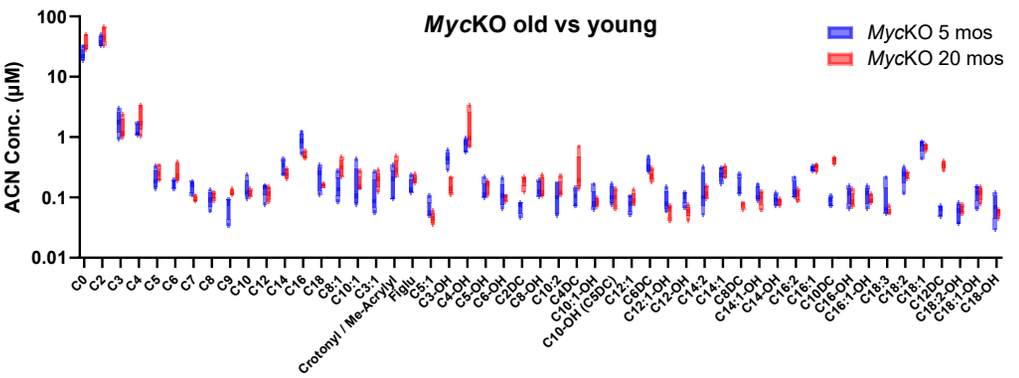

	Below threshold?	P value
C0	Yes *	0.030896
C2	No	0.184339
C3	No	0.361412
C4	No	0.107424
C5	No	0.425804
C6	Yes *	0.041003
C7	Yes **	0.005872
C8	No	0.415367
C9	Yes **	0.003738
C10	No	0.355998
C12	No	0.370061
C14	No	0.083011
C16	Yes *	0.011845
C18	No	0.150392
C8:1	Yes *	0.018524
C10:1	No	0.958586
C3:1	No	0.135059

	Below threshold?	P value
Crotonyl / Me-Acrylyl	No	0.084518
Figlu	No	0.092821
C5:1	No	0.129585
C3-OH	Yes ***	0.000969
C4-OH	No	0.177247
C5-OH	No	0.446142
C6-OH	No	0.554716
C2DC	Yes ***	0.000204
C8-OH	No	0.742848
C10:2	No	0.419328
C4DC	No	0.111577
C10:1-OH	No	0.622889
C10-OH (C5DC)	No	0.594450
C12:1	No	0.389429
C6DC	Yes *	0.048989
C12:1-OH	No	0.089490
C12-OH	Yes **	0.005306

	Below threshold?	P value
C14:2	No	0.590118
C14:1	No	0.502287
C8DC	Yes **	0.009042
C14:1-OH	No	0.281853
C14-OH	No	0.377949
C16:2	No	0.263590
C16:1	No	0.453775
C10DC	Yes ****	<0.000001
C16-OH	No	0.345020
C16:1-OH	No	0.325627
C18:3	No	0.302453
C18:2	No	0.995663
C18:1	No	0.610594
C12DC	Yes ****	<0.000001
C18:2-OH	No	0.521089
C18:1-OH	No	0.967776
C18-OH	No	0.311576

Figure S5. Both young and old WT and *Myc*KO mice show evidence of age-related differences in serum acyl carnitine levels, related to Figure 4F&G

(A). 5 month old and 20 month-old WT mice. Unpaired t test, ∗=p < 0.05, ∗∗=p < 0.01, ∗∗∗=p < 0.001, ∗∗∗∗=p < 0.0001.

(B). 5 month old and 20 month-old *Myc*KO mice. Unpaired t test, ∗=p < 0.05, ∗∗=p < 0.01, ∗∗∗=p < 0.001, ∗∗∗∗=p < 0.0001.

Fig. S6

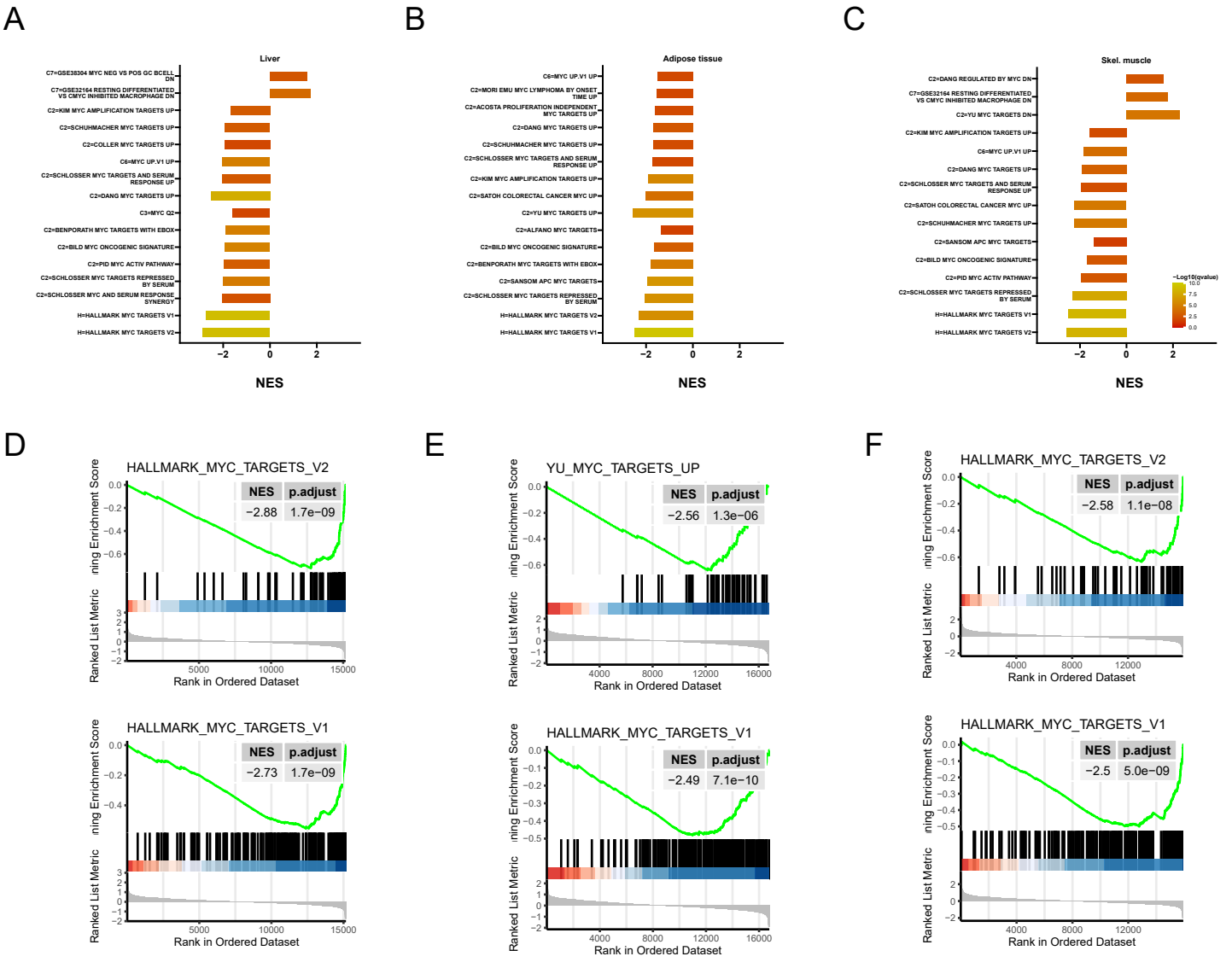
A
Liver
C7=GSE38304 MYC NEG VS POS GC BCELL DN
C7=GSE32164 RESTING DIFFERENTIATED VS CMYC INHIBITED MACROPHAGE DN
C2=KIM MYC AMPLIFICATION TARGETS UP
C2=SCHUHMACHER MYC TARGETS UP
C2=COLLER MYC TARGETS UP
C6=MYC UP.V1 UP
C2=SCHLOSSER MYC TARGETS AND SERUM RESPONSE UP
C2=DANG MYC TARGETS UP
C3=MYC Q2
C2=BENPORATH MYC TARGETS WITH EBOX
C2=BILD MYC ONCOGENIC SIGNATURE
C2=PID MYC ACTIV PATHWAY
C2=SCHLOSSER MYC TARGETS REPRESSED BY SERUM
C2=SCHLOSSER MYC AND SERUM RESPONSE SYNERGY
H=HALLMARK MYC TARGETS V1
H=HALLMARK MYC TARGETS V2
−2
0
2
NES
B
Adipose tissue
C6=MYC UP.V1 UP
C2=MORI EMU MYC LYMPHOMA BY ONSET TIME UP
C2=ACOSTA PROLIFERATION INDEPENDENT MYC TARGETS UP
C2=DANG MYC TARGETS UP
C2=SCHUHMACHER MYC TARGETS UP
C2=SCHLOSSER MYC TARGETS AND SERUM RESPONSE UP
C2=KIM MYC AMPLIFICATION TARGETS UP
C2=SATOH COLORECTAL CANCER MYC UP
C2=YU MYC TARGETS UP
C2=ALFANO MYC TARGETS
C2=BILD MYC ONCOGENIC SIGNATURE
C2=BENPORATH MYC TARGETS WITH EBOX
C2=SANSOM APC MYC TARGETS
C2=SCHLOSSER MYC TARGETS REPRESSED BY SERUM
H=HALLMARK MYC TARGETS V2
H=HALLMARK MYC TARGETS V1
−2
0
2
NES
C
Skel. muscle
C2=DANG REGULATED BY MYC DN
C7=GSE32164 RESTING DIFFERENTIATED VS CMYC INHIBITED MACROPHAGE DN
C2=YU MYC TARGETS DN
C2=KIM MYC AMPLIFICATION TARGETS UP
C6=MYC UP.V1 UP
C2=DANG MYC TARGETS UP
C2=SCHLOSSER MYC TARGETS AND SERUM RESPONSE UP
C2=SATOH COLORECTAL CANCER MYC UP
C2=SCHUHMACHER MYC TARGETS UP
C2=SANSOM APC MYC TARGETS
C2=BILD MYC ONCOGENIC SIGNATURE
C2=PID MYC ACTIV PATHWAY
C2=SCHLOSSER MYC TARGETS REPRESSED BY SERUM
H=HALLMARK MYC TARGETS V1
H=HALLMARK MYC TARGETS V2
−Log10(qvalue)
10.0
7.5
5.0
2.5
0.0
−2
0
2
NES
D
HALLMARK_MYC_TARGETS_V2
NES p.adjust
−2.88 1.7e−09
ning Enrichment Score
Ranked List Metric
Rank in Ordered Dataset
HALLMARK_MYC_TARGETS_V1
NES p.adjust
−2.73 1.7e−09
ning Enrichment Score
Ranked List Metric
Rank in Ordered Dataset
E
YU_MYC_TARGETS_UP
NES p.adjust
−2.56 1.3e−06
ning Enrichment Score
Ranked List Metric
Rank in Ordered Dataset
HALLMARK_MYC_TARGETS_V1
NES p.adjust
−2.49 7.1e−10
ning Enrichment Score
Ranked List Metric
Rank in Ordered Dataset
F
HALLMARK_MYC_TARGETS_V2
NES p.adjust
−2.58 1.1e−08
ning Enrichment Score
Ranked List Metric
Rank in Ordered Dataset
HALLMARK_MYC_TARGETS_V1
NES p.adjust
−2.5 5.0e−09
ning Enrichment Score
Ranked List Metric
Rank in Ordered Dataset

Figure S6. Dysregulation of Myc target gene sets in 5 mo MycKO tissues, related to Figure 1&6.

(A-C). GSEA summaries of positively-regulated direct Myc targets in liver, adipose tissue, and skeletal muscle, respectively from 5 month-old MycKO mice. All Myc targets from the MSigDB Collection (http://www.gsea-msigdb.org/gsea/msigdb/collections.jsp) were analyzed by GSEA to determine the overall directionality of expression of each set's component transcripts.

(D-F). Select examples of individual GSEA profiles from A-C.

Fig. S7

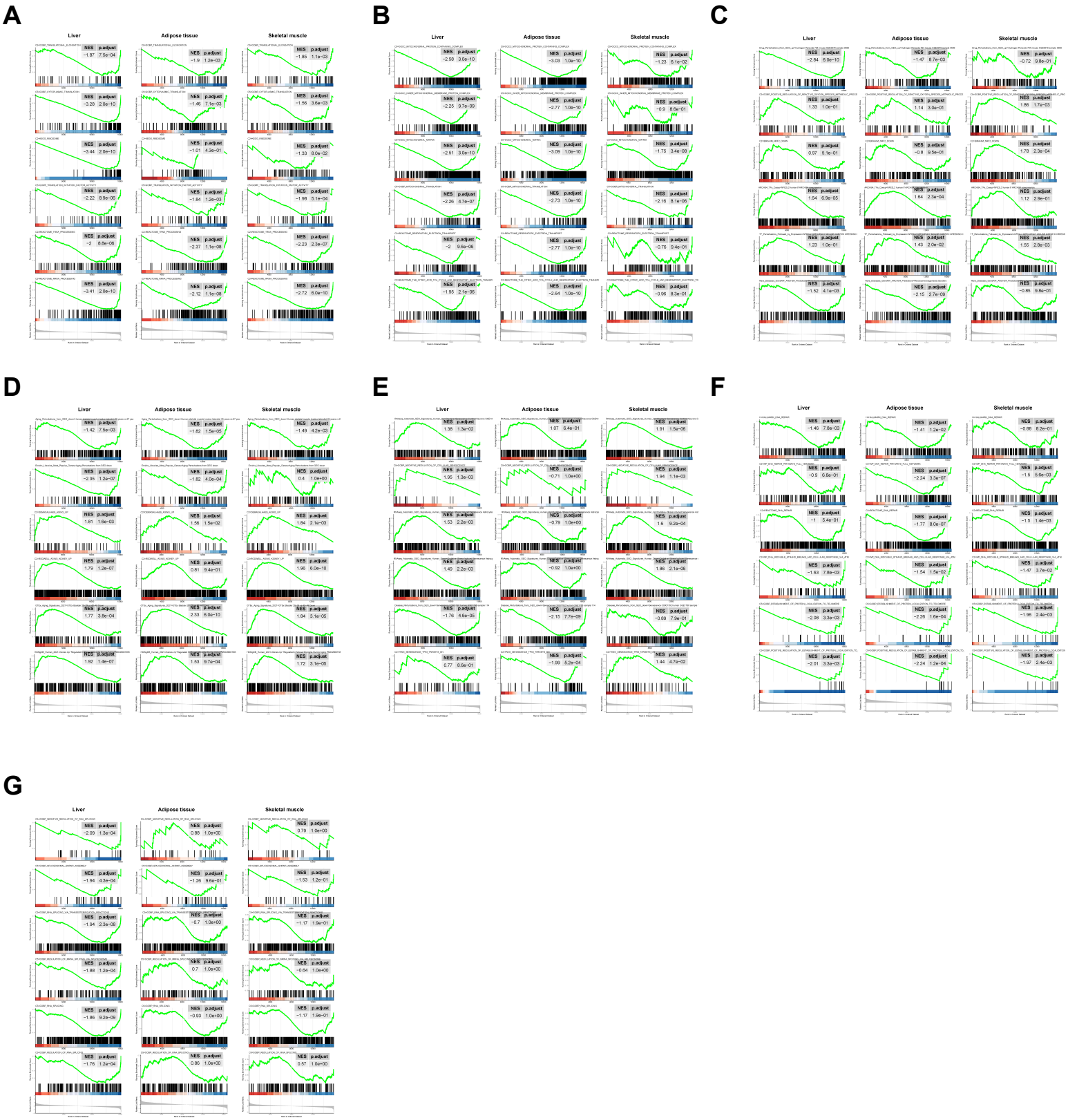

Figure S7. GSEA profiles in liver, adipose tissue and skeletal muscle from 5 month-old WT and MycKO mice, related to Figure 6A. Normalized enrichment scores and q values are indicated in the upper right corner of each profile. Data used to generate the ridge plots shown in Figure 6A are re-graphed and included here**.**

(A) GSEA profiles for “Translation/ribosomal structure and function”.
(B) GSEA profiles for “Mitochondrial structure and function”.
(C) GSEA profiles for “Oxidative stress response”.
(D) GSEA profiles for “Aging”.
(E) GSEA profiles for “Senescence”.
(F) GSEA profiles for “DNA damage response and repair”.
(G) GSEA profiles for “mRNA splicing”.

Fig. S8

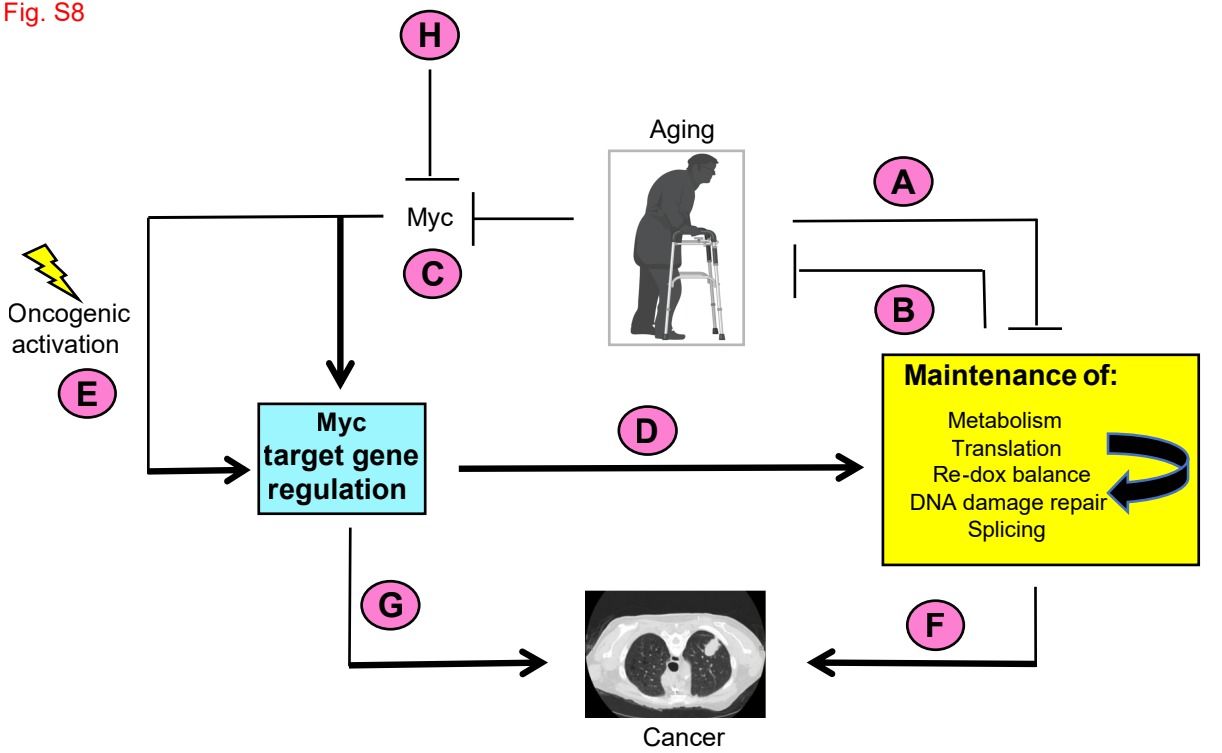
H
Aging
Myc
A
C
B
Oncogenic activation
E
Myc target gene regulation
D
Maintenance of:
Metabolism
Translation
Re-dox balance
DNA damage repair
Splicing
G
F
Cancer

Figure S8. Model depicting the cooperation between normal aging and Myc regulation, related to Figures 1-7 .

(A). Normal aging and senescence are associated with the accumulation of Myc-independent defects involving the maintenance of mitochondrial and ribosomal structure and function, redox balance, DNA damage recognition and repair and splicing (yellow box) (Figure 7A). [4-17] Individual functional defects therein can negatively impact other functions (yellow box: curved arrow). For example, defective mitochondrial function can generate ROS, which in turn can cause oxidative DNA damage and impair translation. [18-22]

(B). Defects in the above functions and pathways conversely accelerate aging. [5,9,11,13,23-26]

(C). Normal aging is also associated with declines in Myc levels, causing dysregulation of Myc target gene expression (blue box) (Figure 7F-I).

(D). Normal levels of Myc and its target genes are needed to maintain the baseline cellular functions depicted in the yellow box. [2,27,28] These cooperate with the age-dependent and Myc-independent pathways shown in A.

(E). Oncogenic activation of Myc can dysregulate Myc target genes, thus altering the functions depicted in the yellow box in ways that sustain maximal rates of tumor growth. [2,27-30]

(F). Dysregulation of the functions described for E and D support the initiation, maintenance and/or evolution of cancer. [27-30]

(G). Other Myc target genes not shown in the yellow box, such as those pertaining to cell cycle and survival, can independently contribute to the development of cancer when they are dysregulated as a result of Myc over-expression. [29,31-33] Some of these genes may be so-called “pathological targets” that contain low-affinity Myc binding sites and are only activated in response to the excessive levels of Myc associated with certain tumors. [29,34]

(H). *Myc*KO mice no longer regulate their target genes. As a result, they lose the ability to maintain the functions depicted in the yellow box, thereby hastening the onset of aging via the Myc-dependent pathway that support these functions (B, C and D). Reductions in Myc also eliminate a major age-dependent oncogenic pathway (E), thus leading to a reduced lifetime incidence of cancer (F and G) that contributes to the increased longevity of these mice.

Table S3. Antibodies used for the current studies, related to STAR Methods.

Name of antigen target	Type of antibody	Vendor	Catalog number	dilution	Purpose
Glut 1	Rabbit mAb	Abcam	Ab115730	1:2,000	WB
Glut 2	Rabbit pAb*	Proteintech	20436-1-AP	1:1,000	WB
Glut 4	Mouse mAb	Cell signaling	2213	1:1,000	WB
GAPDH	Mouse mAb	Sigma	G8795	1:10,000	WB
γH2A.X	Rabbit mAb	Abcam	ab81299	1:200	IHF
PDH	Rabbit mAb	Cell signaling	3205	1:1,000	WB
c-Myc	Rabbit mAb	Cell signaling	13987	1:1,000 1:400	WB
c-Myc(N-262)	Rabbit pAb	Santa Cruze	sc-764	1:250	IHC
p-PDH	Rabbit pAb	Cal biochem	AP1062	1:300	WB
PFK-L	Rabbit pAb	Avivva sys bio	ARP45774_T100	1:400	WB
PFK-M	Mouse mAb	R+D systems	MAB7687	1:3,000	WB
IgG	HRP-Goat-anti-rabbit	Cell signaling	7074	1:5,000 1:2,000	Secondary for WB
IgG	HRP-Goat-anti-mouse	Cell signaling	7076	1:10,000	Secondary for WB

*pAb=Polyclonal antibody

References

1. Wang, H., Dolezal, J.M., Kulkarni, S., Lu, J., Mandel, J., Jackson, L.E., Alencastro, F., Duncan, A.W., and Prochownik, E.V. (2018). Myc and ChREBP transcription factors cooperatively regulate normal and neoplastic hepatocyte proliferation in mice. J Biol Chem *293*, 14740-14757. 10.1074/jbc.RA118.004099.
2. Wang, H., Stevens, T., Lu, J., Airik, M., Airik, R., and Prochownik, E.V. (2022). Disruption of Multiple Overlapping Functions Following Stepwise Inactivation of the Extended Myc Network. Cells *11*. 10.3390/cells11244087.
3. Muncan, V., Sansom, O.J., Tertoolen, L., Phesse, T.J., Begthel, H., Sancho, E., Cole, A.M., Gregorieff, A., de Alboran, I.M., Clevers, H., and Clarke, A.R. (2006). Rapid loss of intestinal crypts upon conditional deletion of the Wnt/Tcf-4 target gene c-Myc. Mol Cell Biol *26*, 8418-8426. 10.1128/MCB.00821-06.
4. Anisimova, A.S., Alexandrov, A.I., Makarova, N.E., Gladyshev, V.N., and Dmitriev, S.E. (2018). Protein synthesis and quality control in aging. Aging (Albany NY) *10*, 4269-4288. 10.18632/aging.101721.
5. Balaban, R.S., Nemoto, S., and Finkel, T. (2005). Mitochondria, oxidants, and aging. Cell *120*, 483-495. 10.1016/j.cell.2005.02.001.
6. Bhadra, M., Howell, P., Dutta, S., Heintz, C., and Mair, W.B. (2020). Alternative splicing in aging and longevity. Hum Genet *139*, 357-369. 10.1007/s00439-019-02094-6.
7. Bratic, A., and Larsson, N.G. (2013). The role of mitochondria in aging. J Clin Invest *123*, 951-957. 10.1172/JCI64125.
8. Deschenes, M., and Chabot, B. (2017). The emerging role of alternative splicing in senescence and aging. Aging Cell *16*, 918-933. 10.1111/acel.12646.
9. Edgar, D., Shabalina, I., Camara, Y., Wredenberg, A., Calvaruso, M.A., Nijtmans, L., Nedergaard, J., Cannon, B., Larsson, N.G., and Trifunovic, A. (2009). Random point mutations with major effects on protein-coding genes are the driving force behind premature aging in mtDNA mutator mice. Cell Metab *10*, 131-138. 10.1016/j.cmet.2009.06.010.
10. Gonskikh, Y., and Polacek, N. (2017). Alterations of the translation apparatus during aging and stress response. Mech Ageing Dev *168*, 30-36. 10.1016/j.mad.2017.04.003.
11. Jang, J.Y., Blum, A., Liu, J., and Finkel, T. (2018). The role of mitochondria in aging. J Clin Invest *128*, 3662-3670. 10.1172/JCI120842.
12. Meshorer, E., and Soreq, H. (2002). Pre-mRNA splicing modulations in senescence. Aging Cell *1*, 10-16. 10.1046/j.1474-9728.2002.00005.x.
13. Opresko, P.L., and Shay, J.W. (2017). Telomere-associated aging disorders. Ageing Res Rev *33*, 52-66. 10.1016/j.arr.2016.05.009.
14. Park, Y., and Gerson, S.L. (2005). DNA repair defects in stem cell function and aging. Annu Rev Med *56*, 495-508. 10.1146/annurev.med.56.082103.104546.
15. Short, K.R., Bigelow, M.L., Kahl, J., Singh, R., Coenen-Schimke, J., Raghavakaimal, S., and Nair, K.S. (2005). Decline in skeletal muscle mitochondrial function with aging in humans. Proc Natl Acad Sci U S A *102*, 5618-5623. 10.1073/pnas.0501559102.
16. Srivastava, S. (2017). The Mitochondrial Basis of Aging and Age-Related Disorders. Genes (Basel) *8*. 10.3390/genes8120398.
17. Turi, Z., Lacey, M., Mistrik, M., and Moudry, P. (2019). Impaired ribosome biogenesis: mechanisms and relevance to cancer and aging. Aging (Albany NY) *11*, 2512-2540. 10.18632/aging.101922.
18. Ghosh, A., and Shcherbik, N. (2020). Effects of Oxidative Stress on Protein Translation: Implications for Cardiovascular Diseases. Int J Mol Sci *21*. 10.3390/ijms21082661.

19. Kirkinezos, I.G., and Moraes, C.T. (2001). Reactive oxygen species and mitochondrial diseases. Semin Cell Dev Biol *12*, 449-457. 10.1006/scdb.2001.0282.
20. Molenaars, M., Janssens, G.E., Williams, E.G., Jongejan, A., Lan, J., Rabot, S., Joly, F., Moerland, P.D., Schomakers, B.V., Lezzerini, M., et al. (2020). A Conserved Mito-Cytosolic Translational Balance Links Two Longevity Pathways. Cell Metab *31*, 549-563 e547. 10.1016/j.cmet.2020.01.011.
21. Rosca, M.G., Vazquez, E.J., Chen, Q., Kerner, J., Kern, T.S., and Hoppel, C.L. (2012). Oxidation of fatty acids is the source of increased mitochondrial reactive oxygen species production in kidney cortical tubules in early diabetes. Diabetes *61*, 2074-2083. 10.2337/db11-1437.
22. Vafa, O., Wade, M., Kern, S., Beeche, M., Pandita, T.K., Hampton, G.M., and Wahl, G.M. (2002). c-Myc can induce DNA damage, increase reactive oxygen species, and mitigate p53 function: a mechanism for oncogene-induced genetic instability. Mol Cell *9*, 1031-1044. 10.1016/s1097-2765(02)00520-8.
23. Kauppila, T.E.S., Kauppila, J.H.K., and Larsson, N.G. (2017). Mammalian Mitochondria and Aging: An Update. Cell Metab *25*, 57-71. 10.1016/j.cmet.2016.09.017.
24. Lenaz, G., Bovina, C., Castelluccio, C., Fato, R., Formiggini, G., Genova, M.L., Marchetti, M., Pich, M.M., Pallotti, F., Parenti Castelli, G., and Biagini, G. (1997). Mitochondrial complex I defects in aging. Mol Cell Biochem *174*, 329-333.
25. Stefanatos, R., and Sanz, A. (2011). Mitochondrial complex I: a central regulator of the aging process. Cell Cycle *10*, 1528-1532. 10.4161/cc.10.10.15496.
26. Trifunovic, A., and Larsson, N.G. (2008). Mitochondrial dysfunction as a cause of ageing. J Intern Med *263*, 167-178. 10.1111/j.1365-2796.2007.01905.x.
27. Dang, C.V., O'Donnell, K.A., Zeller, K.I., Nguyen, T., Osthus, R.C., and Li, F. (2006). The c-Myc target gene network. Semin Cancer Biol *16*, 253-264. 10.1016/j.semcancer.2006.07.014.
28. Dolezal, J.M., Wang, H., Kulkarni, S., Jackson, L., Lu, J., Ranganathan, S., Goetzman, E.S., Bharathi, S.S., Beezhold, K., Byersdorfer, C.A., and Prochownik, E.V. (2017). Sequential adaptive changes in a c-Myc-driven model of hepatocellular carcinoma. J Biol Chem *292*, 10068-10086. 10.1074/jbc.M117.782052.
29. Prochownik, E.V. (2022). Regulation of Normal and Neoplastic Proliferation and Metabolism by the Extended Myc Network. Cells *11*. 10.3390/cells11243974.
30. Shachaf, C.M., Kopelman, A.M., Arvanitis, C., Karlsson, A., Beer, S., Mandl, S., Bachmann, M.H., Borowsky, A.D., Ruebner, B., Cardiff, R.D., et al. (2004). MYC inactivation uncovers pluripotent differentiation and tumour dormancy in hepatocellular cancer. Nature *431*, 1112-1117. 10.1038/nature03043.
31. Dang, C.V. (2011). Therapeutic targeting of Myc-reprogrammed cancer cell metabolism. Cold Spring Harb Symp Quant Biol *76*, 369-374. 10.1101/sqb.2011.76.011296.
32. Dang, C.V. (2012). MYC on the path to cancer. Cell *149*, 22-35. 10.1016/j.cell.2012.03.003.
33. Gabay, M., Li, Y., and Felsher, D.W. (2014). MYC activation is a hallmark of cancer initiation and maintenance. Cold Spring Harb Perspect Med *4*. 10.1101/cshperspect.a014241.
34. Prochownik, E.V., and Wang, H. (2022). Normal and Neoplastic Growth Suppression by the Extended Myc Network. Cells *11*. 10.3390/cells11040747.